

¹R. Ramani²A. Nalini

Enhanced EV Battery Monitoring Using IoT with Improved SEPIC - ZETA Converter and Modified Lion Optimization for Photovoltaic Systems



Abstract: - The rising popularity of electric vehicles (EVs) and the increasing emphasis on sustainable transportation have highlighted the importance of advanced monitoring systems. These systems play a crucial role in providing real-time information about battery parameters to ensure optimal performance and longevity. Moreover, the integration of renewable energy sources, specifically photovoltaic (PV) systems, with EV charging infrastructure presents an exciting prospect to enhance energy efficiency and minimize environmental harm. As a consequence the proposed work develops an Internet of Things (IoT) based PV fed EV charging system. The system incorporates an improved SEPIC-Zeta converter together with Modified Lion Optimization algorithm (LOA) assisted Proportional Integral (PI) controller for optimizing PV system for charging EV battery. IoT connectivity monitors parameter such as PV voltage, PV current, and State of Charge (SOC) of battery. Real-time monitoring of these parameters is achieved by leveraging sensors. The collected data is transmitted through IoT networks to a central monitoring system, enabling operators to track the performance of PV system and EV battery. This facilitates optimized energy generation, efficient battery charging and discharging, and overall system reliability. IoT-enabled monitoring system provides remote accessibility, data analytics, and the generation of alerts and notifications for timely actions. Experimental validation demonstrates that, the proposed concept enhances the monitoring capabilities, improves energy efficiency, and ensures reliable operation of EV charging infrastructure.

Keywords: Electric vehicles, photovoltaic system, improved SEPIC-Zeta converter, Modified Lion optimization algorithm, Internet of things

I. INTRODUCTION

Due to the fact that they emit no greenhouse gases and do not rely on crude oil producing countries to determine gas prices, EVs are proving to be a viable alternative to hydrocarbon automobiles [1, 2]. Vehicle electrification is a perfect countermeasure to help ease the significant challenges of carbon emissions and energy shortages that modern industrial production and daily living must deal effectively. In a vehicle powered by electricity, a battery monitoring system is essential. It guarantees the longevity of the battery, maintains the battery's functionality, and protects it from harm. To increase battery quality and assure safe operation, battery operating systems are utilized [3, 4]. Over the past 20 years, EV has grown significantly due to this need. EVs are gradually replacing conventional fuel-dependent vehicle, therefore durability and driving safety standards are becoming more and more crucial [5]. By analysing fluctuations in voltage and current entering load profile, nonintrusive load monitoring (NILM) [6] is a means of splitting up collected electric power and current and transforming it into individual appliances. Due to the fact that the output from PV systems is determined by ambient temperature and natural lighting levels, PV-interfaced EV idea necessitates the deployment of an appropriate tracking technique. Hence, converter approaches are involved in this work, to boost the low voltage attained from PV panel.

The Boost converter delivers substantial benefits at high duty ratios but lacks input current control. It uses a high duty cycle to suck some input current from source, which harms the converter's component parts [7]. When compared to boost converters, buck-boost converters are capable of meeting step-up or step-down requirements, but they are inefficient and cannot provide significant gains [8]. The voltage from the input is converted to higher and lower voltage levels in output by means of common single switch step-down/step-up converters like Buck converter, Buck-boost converter [9], Cuk [10, 11], Zeta [12] and Single-Ended Primary Inductance Converter (SEPIC) [13]. In this work, an improved SEPIC-Zeta converter approach is proposed for

^{1,2}Department of Electrical and Electronics Engineering, Dr. M.G.R. Educational and Research Institute, Tamilnadu, India.

*Corresponding Author Email: ramanikamal11@gmail.com

enhancement of PV panel output with high voltage gain and low voltage ripples. To balance and improve energy obtained from PV system, a controller approach and optimization technique is employed after converter operation. PI controllers are one of the methods most frequently used to increase the output of a solar array.

A population-based algorithm called a Genetic Algorithm (GA) makes use of the ideas of biological evolution and the survival of the fittest. Selection, crossover, and mutation [14] are the primary GA operators, making iteration a long, challenging process to comprehend and debug. Particle Swarm Optimization (PSO) algorithm makes use of individual cooperation and information sharing to arrive at the best possible result. Each particle updates its velocity and position by keeping track of both local and global extreme values during each iteration [15], but the algorithm's iteration process has a relatively slow convergence rate. Whale Optimization Algorithm (WOA) is a meta-heuristic optimization algorithm that mimics foraging strategies of humpback whales [16], however it struggles to identify the overall best solution to very complicated, high-dimensional optimization problems. In this work, modified LOA is proposed because it determines solution that consistently minimizes cost function irrespective the size of solution spaces, i.e., it minimized the cost function. The retained DC voltage is delivered to the grid by means of a 1ϕ VSI. The LC filter [17] has been employed to minimize the system's harmonics, which enhances the stability of the system [18].

The main benefactions proposed in this work are listed in the following;

- To create an effective PV fed EV battery system based on RES, which aims to lessen both the problem of global warming and overdependence on fossil fuels.
- To step up the voltage obtained from PV panel to desired level, improved SEPIC-Zeta converter approach is employed.
- To maintain a steady voltage supply, improved SEPIC-Zeta converter and modified LOA-assisted PI controller is employed for better efficiency.
- To visualize the parameters like PV voltage, current and SOC of battery, IoT display is utilized.

Overall system is executed in MATLAB platform and based on the outcomes obtained, better working of the system is verified.

II. PROPOSED SYSTEM DESCRIPTION

Energy from the sun is capable of being used during the day to charge EVs from renewable energy sources, which promotes the growth of clean energy and lowers greenhouse gas emissions. In this work, a grid-integrated PV system with an EV battery monitoring system using IoT is proposed in order to track parametric data like SOC, I_{PV} and V_{PV} . Figure 1 illustrates the schematic diagram for proposed system.

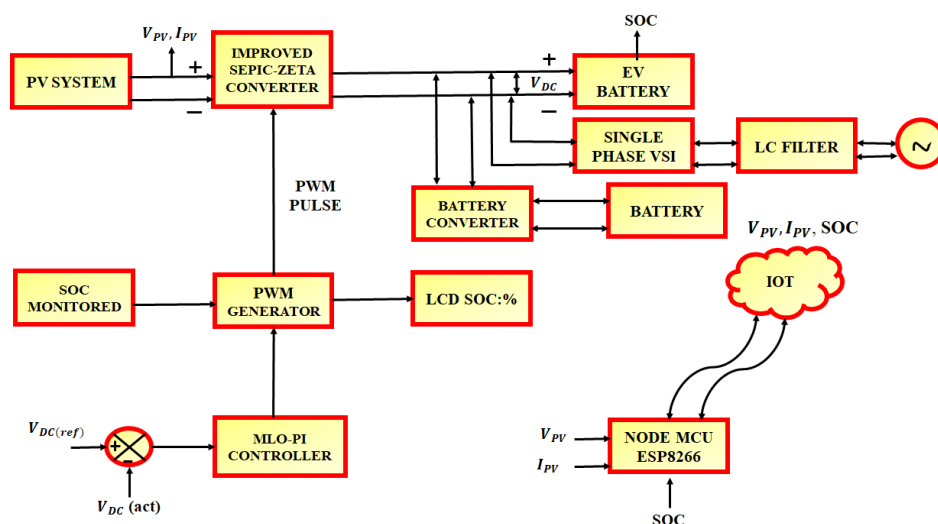


Figure 1: Schematic diagram of proposed system

The output obtained from PV system is intermittent due to effects of temperature variation and solar irradiation and this energy is not sufficient to power the grid. Hence, a DC-DC converter is required in enhancement of voltage supplied to grid. In this work, improved SEPIC-Zeta converter is proposed, in which it is controlled using MLO-PI controller approach. The reference and actual DC voltage is compared and the obtained error signal is fed into MLO-PI controller. Then output from controller is fed into PWM generator, which generates PWM pulses for working of improved SEPIC-Zeta converter. The energy is then stored in EV battery for further use of proposed system. The DC link voltage is then converted into AC voltage using 1ϕ VSI and then fed into LC filter in which harmonics are eliminated from AC supply. The battery converter is utilized for converting the AC power into DC supply and then stored in battery. The significant parameters that influences the working of proposed system such as I_{PV} , V_{PV} and SOC of battery are monitored using IoT display. The modelling of proposed system is explained in the following.

III. PROPOSED SYSTEM MODELLING

i) PV SYSTEM

For attaining optimum voltages and current levels, numerous solar cells are connected in series and parallel to form a PV module. A p-n semiconductor junction is essentially makes up a solar cell, thereby a direct current is produced when exposed to light. The circuit for PV panel is constructed using a diode, series resistance (R_s) because of its contacts between metal part and semiconductors, a photo current (I_{ph}) and resistance which is connected parallel (R_p) that indicates a current leakage as illustrated in Figure 2.

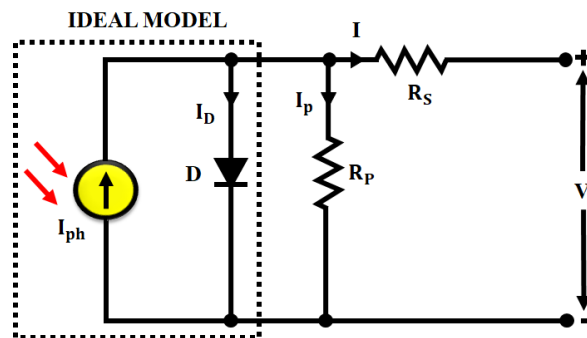


Figure 2: Equivalent circuit for PV cell

The current equation is obtained by Kirchoff's law,

$$I = I_{ph} - I_D - I_p \quad (1)$$

Where I_p which is current through parallel resistor and I_{ph} is current produced by photocurrent or light that is determined as;

$$I_p = \frac{V + R_s I}{R_p} \quad (2)$$

The current through diode which is represented as I_D that is proportional to saturation current. The magnitude of diode current is represented as follows,

$$I_D = I_{sd} \left(\exp \left(\frac{q(V + R_s I)}{n.K.T} \right) - 1 \right) \quad (3)$$

Where I_{sd} reverse saturation is current denoted in amperes (A), K denotes Boltzmann constant ($1.38 \times 10^{-23} \text{J/K}$). The obtained PV voltage is reduced due to climatic conditions, hence a converter approach is required to boost up voltage to power the grid and following section explains the converter approach utilized in this work.

ii) IMPROVED SEPIC-ZETA CONVERTER

The SEPIC-Zeta converter compared to a traditional Boost converter, it is a voltage-boosting converter which provides a quick transient response. However, selecting an improved design increases voltage gain of SEPIC-Zeta converter. The improved converter consists of two inductors L_1 and L_2 , two switches S_1 and S_2 , capacitors C_1 and C_2 along with output capacitor C_0 , two diodes D_1 and D_2 and resistor R . Figure 3 illustrates design for improved SEPIC-Zeta converter. Figure 5 represents waveform for working of proposed converter in two different modes.

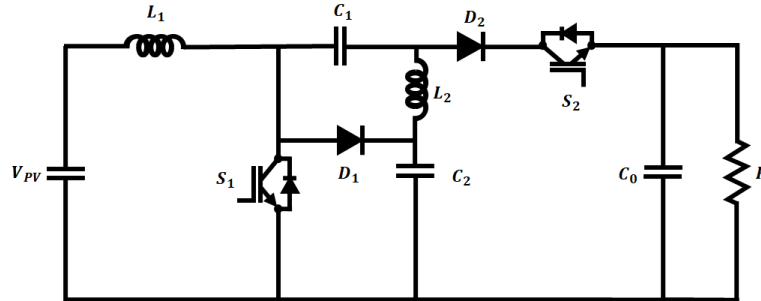


Figure 3: Improved SEPIC-Zeta Converter

The following section explains operations of converter in two different modes;

Mode 1 [t_1, t_2]: In this mode, Switch S_1 is kept in ON condition in which Switch S_2 and diodes D_1 and D_2 are kept in OFF condition. Across the two inductor, current flow is indicated as i_{L1} and i_{L2} and input voltage V_{spk} determines the point at which the output current increases gradually, which is stated in equation (4),

$$\frac{di_{L1}}{dt} = \frac{di_{L2}}{dt} = \frac{V_{spk}}{L_1(=L_2)} \quad (4)$$

Mode 2 [t_2, t_3]: In this mode, Switch S_2 is kept in ON condition in which the Switch S_1 is switched OFF. Two diodes D_1 and D_2 starts to conduct, whereas the two inductors L_1 and L_2 supplies the energy stored to the Zeta converter through diode D_2 . The representation for the current from inductor is given as,

$$\frac{di_{L1}}{dt} = \frac{di_{L2}}{dt} = \frac{V_{spk} - V_{dc} + V_{C1}}{2L_1(=L_2)} \quad (5)$$

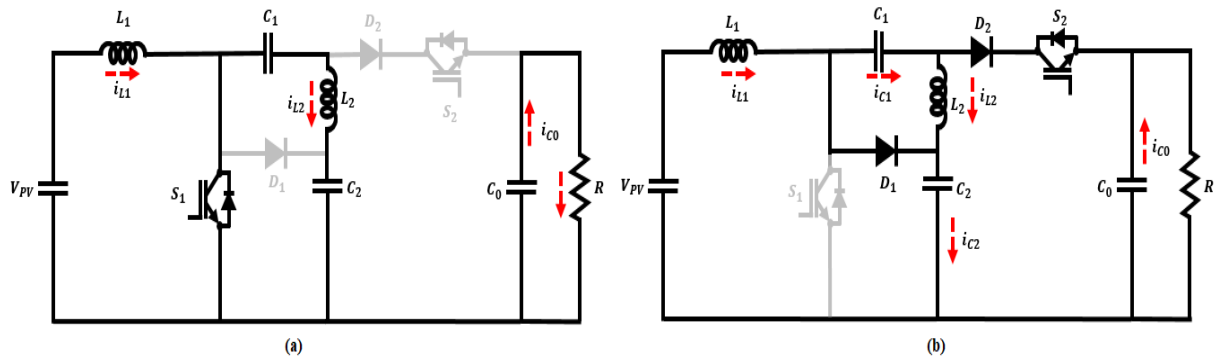


Figure 4: Modes of operation (a) Mode 1 (b) Mode 2

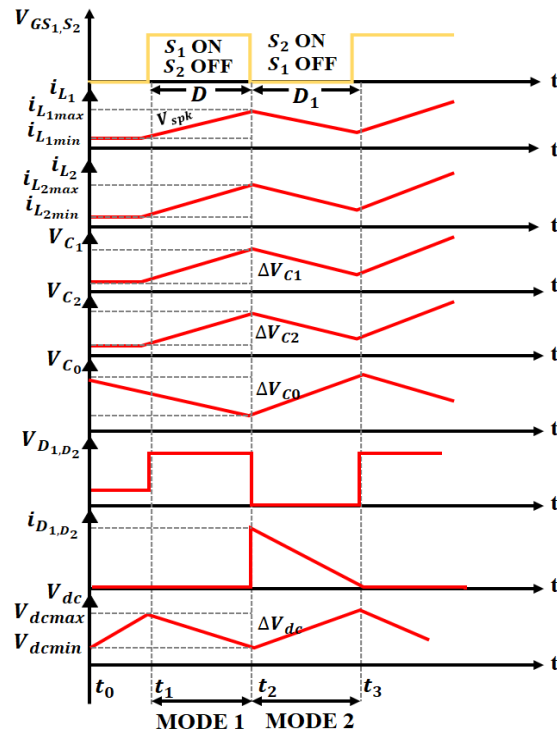


Figure 5: Timing diagram for proposed converter

The output voltage is greater than input voltage, it responds quickly to rapid load changes, has a low voltage ripple, and has good precision. This converter is additionally useful in industrial settings because it is straightforward to develop and maintain. The optimization technique utilized in this work is explained in the following.

iii) MODIFIED LION OPTIMIZATION ALGORITHM

The social behavior of the strongest animal on Earth, the lion, is the basis of LOA, as it locates an optimal or nearly optimal solution to the issue. However, there is an inadequate design procedure and an issue in deciding whether to give flexible or competitive interactions. Hence, a Modified LOA, which is a bio-inspired based on population’s optimization approach that incorporates the socio-behavioural of lion species is proposed in this work and flowchart for Modified LOA is illustrated in Figure 6. In order to solve constraint fulfillment problem, following approach concentrates on the mathematical modelling of lions' social organization, mating behavior, and survival. The socio-behavioural interpretation of lions in a population will be modelled as an algorithm to get the overall or workable solution from a vast search space. Every potential solution, according to Yazdani and Jolai (2016), is represented as a Lion dwelling in a certain jungle. As a result, lion represents bipolar interpretation that hybrid model will compute. The procedure for implementing modified LOA is listed below;

1. Creating a pride generation

The pride generation is created and it is represented as L_{ij} and 100 lions are initialized.

$$L_{ij} = \begin{cases} 1 & rand(0,1) \geq 0.5 \\ -1 & Otherwise \end{cases} \quad 1 \leq i \leq N, 1 \leq j \leq 100, \quad (6)$$

2. Calculation for fitness

The fitness value is calculated for lions and it is altered based on the requirement of the proposed work.

$$fitness_i = \sum_{i=1, j=1}^{NC} C_{ij} \quad (7)$$

3. Process of Hunting

The lion will be split into an attacking lion and a hunter lion at random. According to Yazdani and Jolai, the lion with a greater level of fitness is more likely to become a hunting lion.

$$Prey' = Prey + rand(0,1) \times PI \times (Prey - Hunter) \quad (8)$$

Where *Hunter* denotes hunter lion, *Prey* is a prey lion and *PI* indicates improvement in percentage fitness of hunter

4. Achieving a safe environment

The LOA is designed to preserve the most effective answers found through iteration because each pride's enclave consists of each member's best individual positions.

5. Wandering Procedure

The probability of the solution enhancement will be evaluated at this stage before it is elected to the next stage.

$$pr_i = 0.1 + \min\left(0.5, \frac{(Nomad_i - Best_{Nomad})}{Best_{Nomad}}\right) \quad i = 1, 2, 3 \dots \quad (9)$$

Where $Nomad_i$ represents current position, pr_i indicates roaming probability and $Best_{Nomad}$ indicates best nomad lion's fitness.

6. Pairing up

During mating, cross-overs, mutations, and gender grouping all contribute to determining the best solution. Nomadic lions will be the descendants of the offspring.

$$L_{offspring} = \beta \times L_{female} + \sum \frac{(1-\beta)}{\sum_{i=1}^{NR} S_i} \times L_{males} \times S_i \quad (10)$$

Where NR denotes nomadic male lions count, value of S_i is kept as 1, parameters generated randomly with in (0, 1) is denoted as β and $L_{offspring}$ denotes the number of generated offspring's.

7. Defense of the territory

The territorial protection process evaluates both current possibilities (the territorial lion) and newly emerging ones (the nomadic lion). Therefore, if the freshly developed alternative has a greater fitness than the present solution, it will be promoted to be current solution.

8. Invasion of territory

This operator is the same as the selection in the vast majority of algorithms that were influenced by nature. Equation (11), then, will be used to choose the best lion or lioness; if not, move on to Step 3.

$$fitness_i = \max\{NC\} \quad (11)$$

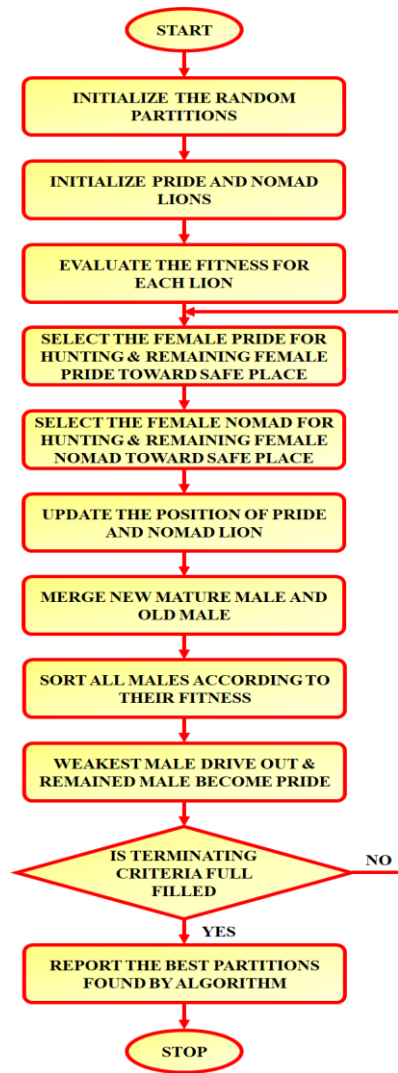


Figure 6: Flowchart for MLO algorithm

IV. RESULTS AND DISCUSSION

The improved SEPIC-Zeta converter approach for enhancing the PV system's productivity is presented in this work. As a result, PWM generator and MLO-based PI controller function together to provide DC link with stabilized voltage to grid. Utilizing IoT, the proposed grid-tied PV system architecture is continually monitored with the goal of enhancing system performance and reliability. Table 1 illustrates the specifications utilized for parameters in this work.

Table 1. Parameter Specifications

Parameter	Specifications
<i>Solar PV panel</i>	
Series connected Solar PV Cells	36
Short Circuit Current	8.3A
Peak Power	10KW
Open circuit Voltage	12V
<i>Improved SEPIC-Zeta converter</i>	
C_1, C_2, C_0	25 μ F
L_1, L_2	5mH
Switching Frequency	10kHz

The waveform for solar panel outputs are depicted in Figure 7. The temperature waveform for solar panel shown in Figure 7(a), initially temperature is maintained at 25°C till 0.1s, after that it is increased to 35°C and constantly maintained throughout the system. The irradiation waveform for solar panel is shown in Figure 7(b), which details about performance of solar panel is observed by changing from 800 W/m² to 1000 W/m². Initially voltage is observed at 40V till 0.1s and after that voltage is increased to 55V and it is maintained constant throughout the system as depicted in Figure 7(c). The current waveform shown in Figure 7(d) details that current is raised above 7A in the beginning and it is maintained constant at 2.3A throughout the system.

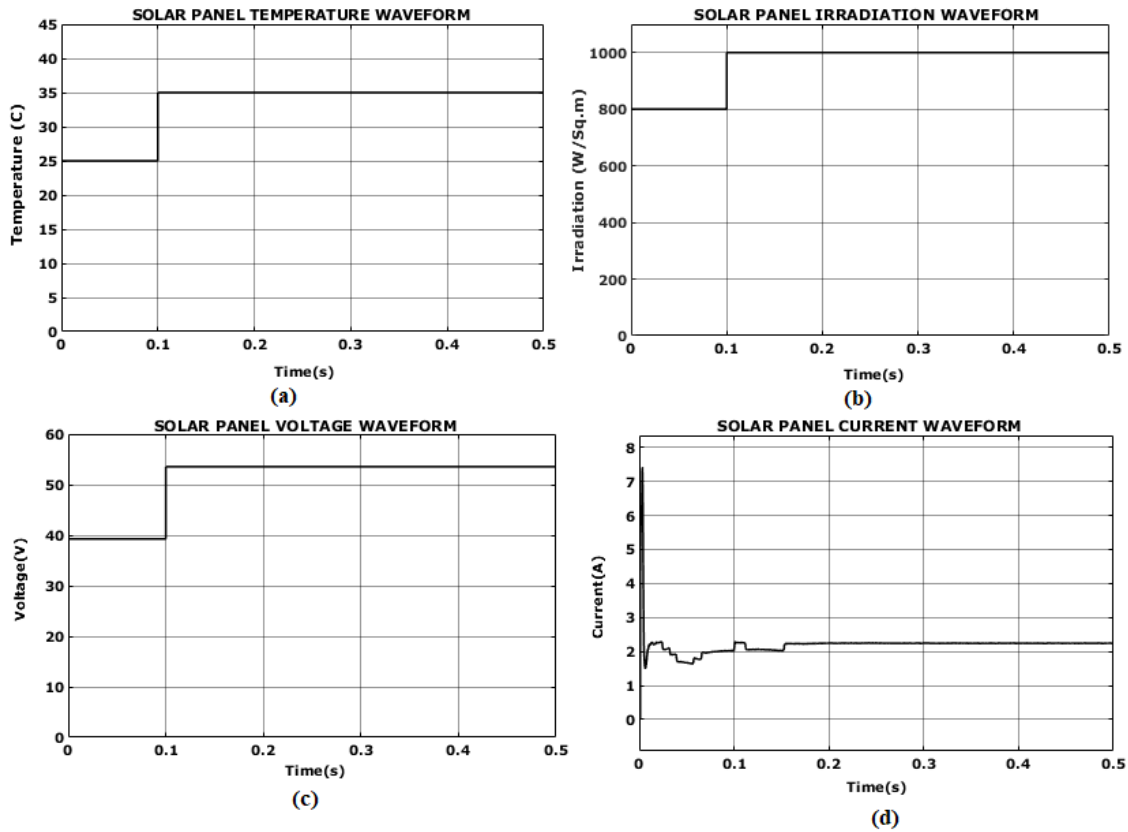


Figure 7: Solar Panel waveforms (a) Temperature (b) Irradiation (c) Voltage (d) Current

The waveforms for converter operation is illustrate in Figure 8. Using PI controller approach, converter waveform for output voltage is depicted in Figure 8(a), which indicates that initially the voltage is increased above 400V and it is maintained constantly at 300V with minor distortion. The output voltage of converter using MLO-PI controller approach is shown in Figure 8(b), in which the voltage is raised to peak above 350V and it is maintained at 330V throughout the system. The output current of converter is shown in Figure 8(c), in which current is fluctuated positively and negatively in the beginning and then it is maintained constantly at 2A throughout the system.

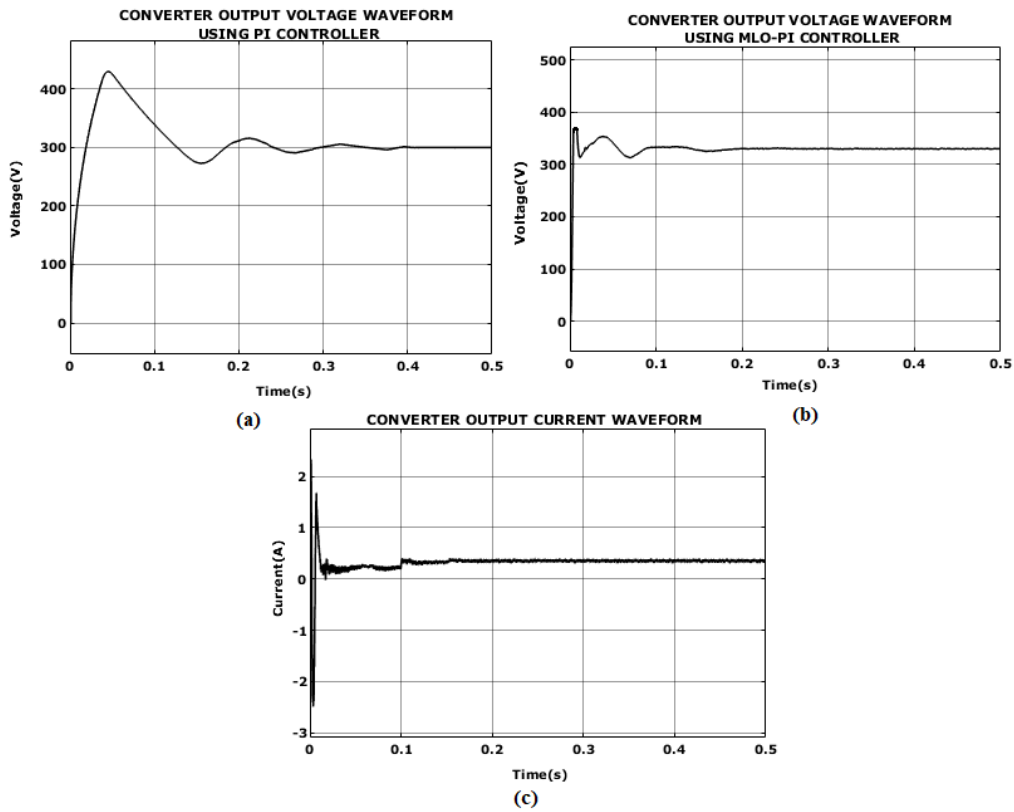


Figure 8: Converter waveforms (a) Output voltage using PI controller (b) Output voltage using MLO-PI controller (c) Output current

The waveforms for battery is illustrated in Figure 9. The voltage waveform for battery is depicted in Figure 9(a), details that voltage is maintained constantly at 24V throughout the system. The current waveform for battery is illustrated in Figure 9(b), in which current is maintained constantly at 1.5A with minor distortions throughout the system. The waveform for Battery State of Charge (SOC) is depicted in Figure 9(c), details that 70% of charge is stored in battery obtained from solar panel.

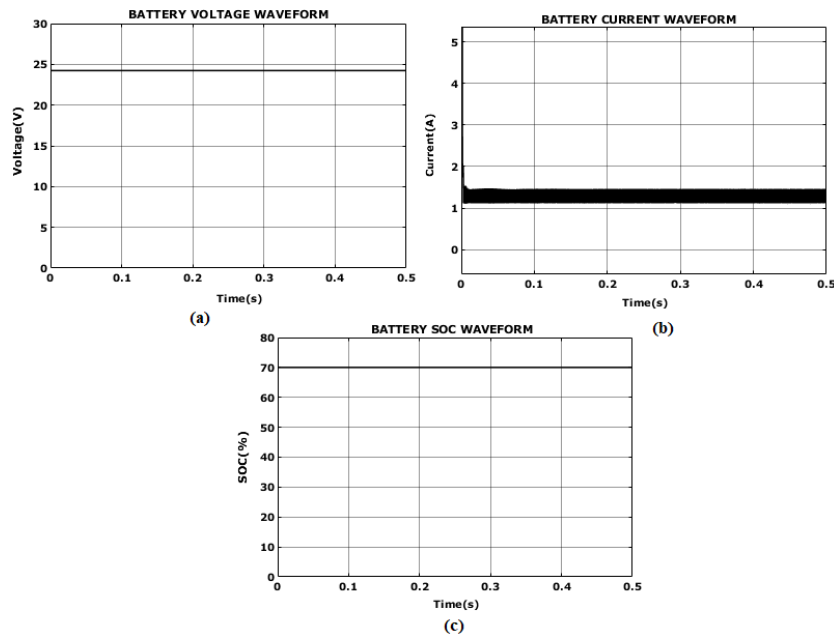


Figure 9: Battery waveforms (a) Voltage (b) Current (c) SOC

The waveforms for grid is shown in Figure 10. From the voltage waveform for grid shown in Figure 10(a), which indicates that the voltage is maintained within the range of ± 230 . The grid current waveform is shown in Figure 10(b), in which the current is maintained within the range of $\pm 5A$ throughout the system.

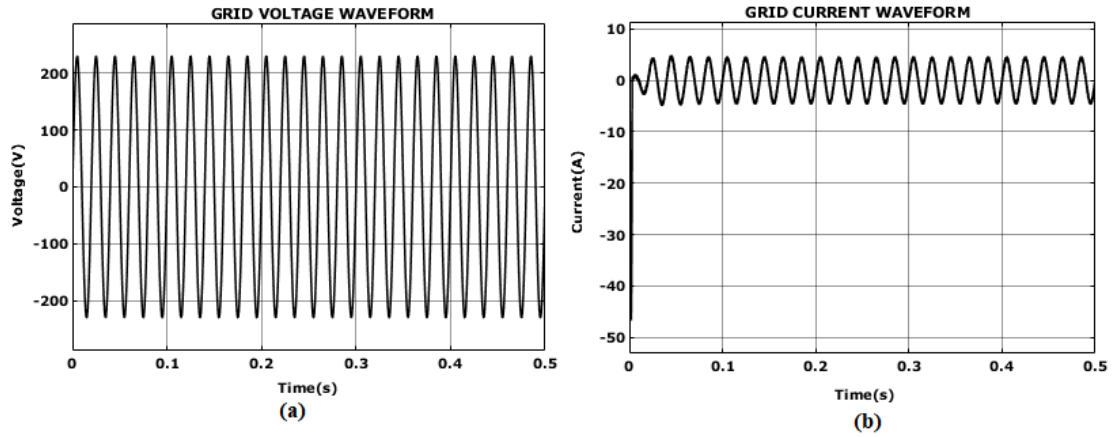


Figure 10: Grid waveforms (a) Voltage (b) Current

The waveforms for real, reactive power and power factor is displayed in Figure 11. Using the proposed system, unity power factor is attained after 0.1s.

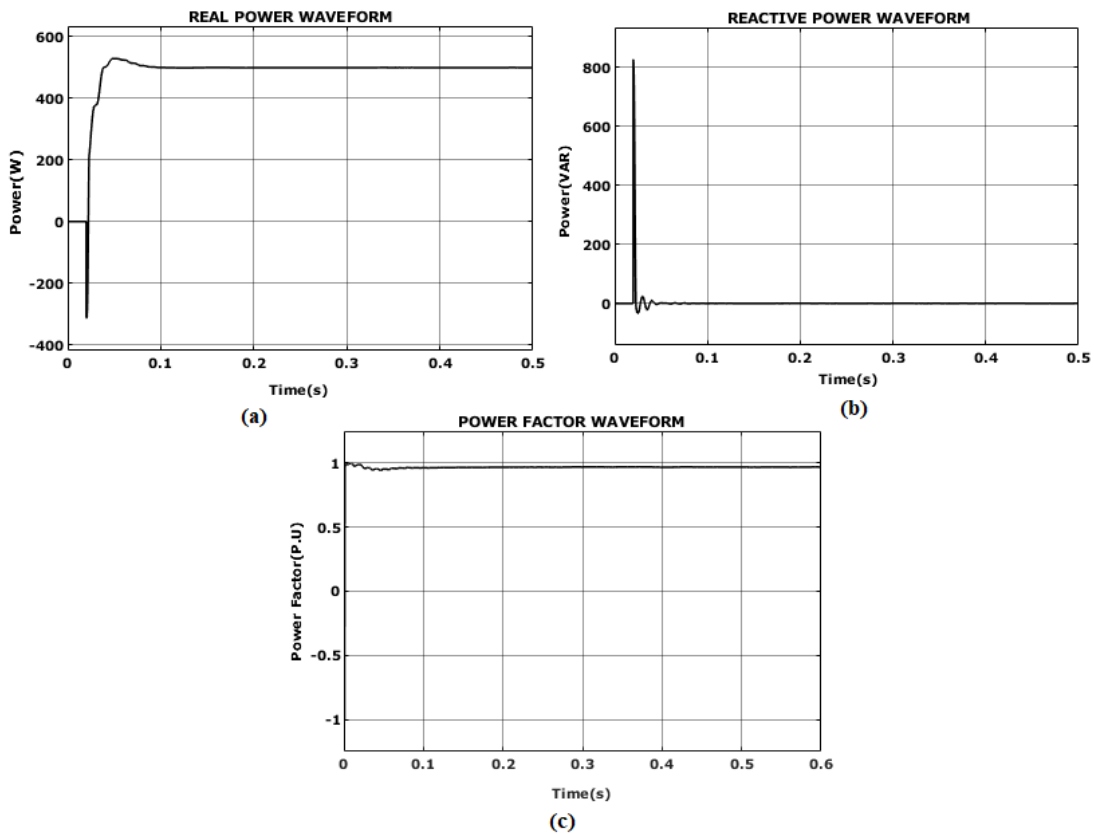


Figure 11: Waveforms for (a) Real power (b) Reactive Power (c) Power factor

The enhanced battery performance monitored using IoT display for the proposed system is illustrated in Figure 12. The output is displayed for voltage and current of solar panel along with SOC of battery.

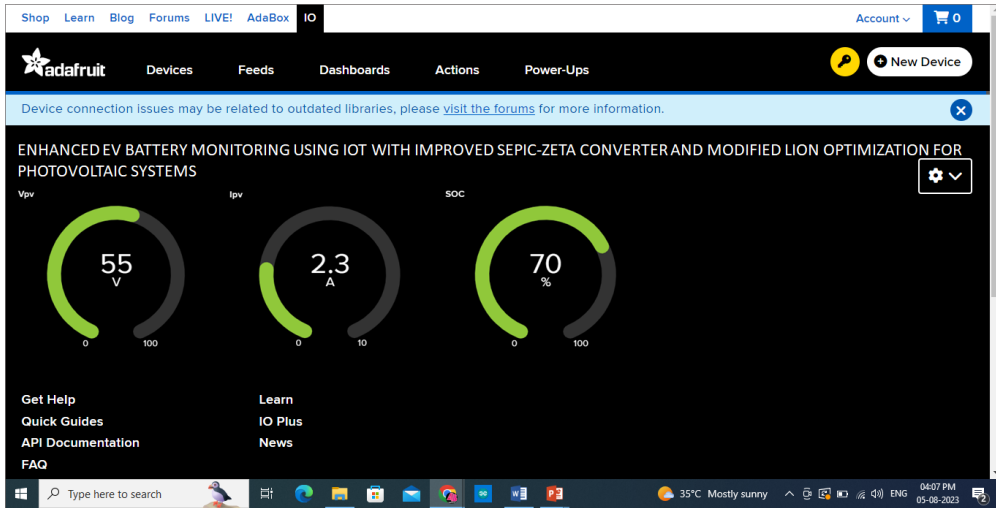


Figure 12: IoT result

The visual representation of THD value is shown in Figure 13, displays a graphic representation of total harmonic distortion (THD). The grid current THD resulting from the proposed work is 1.89%, as it is observed in the depiction, and it serves as a clue as to the distortion that happened in the waveform.

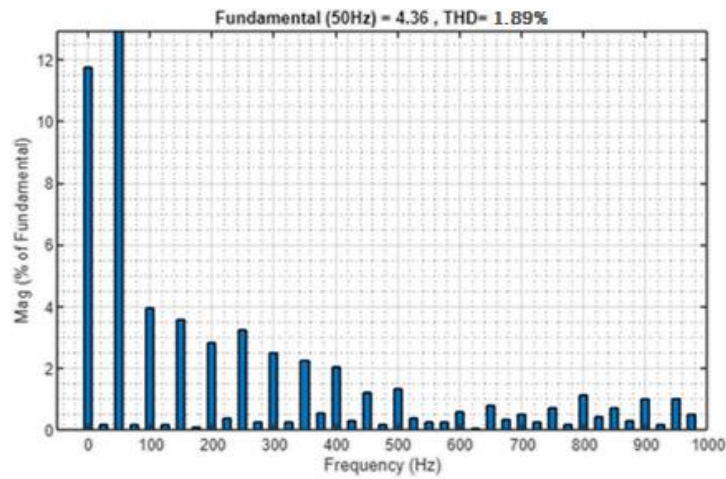


Figure 13: THD waveform

The comparison for settling time for different controller approaches is shown in Figure 14 and Table 2, which details that the proposed control approach has less settling time with 0.2s when compared to other techniques.

Table 2. Comparison analysis for settling time of controller approaches

Control approaches	Settling Time (s)	Rise Time (s)
PI	0.45	0.15
LOA-PI	0.35	0.18
Modified LOA-PI	0.2	0.25

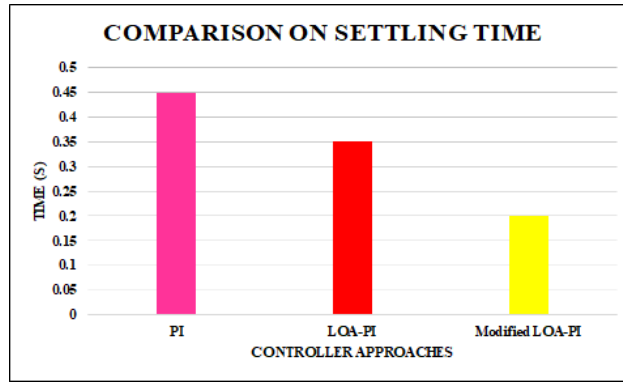


Figure 14: Comparison on settling time of controllers

The comparative analysis on efficiency and voltage gain for different converters are illustrated in Table 3 and visual representation for analysis is shown in Figure 15. From comparison it is detailed that proposed improved SEPIC-Zeta converter has better efficiency with 97% and voltage gain with 1:13 is obtained and it verifies the better working of the proposed system.

Table 3. Comparative Analysis on Efficiency, Voltage Gain and THD values of different converters

Converters	Efficiency	Voltage Gain	THD (%)
Boost	80 [19]	1.5	2.99
SEPIC	88.82[20]	8	2.3
Zeta	90 [21]	9	2
Improved SEPIC-Zeta	97	13	1.89

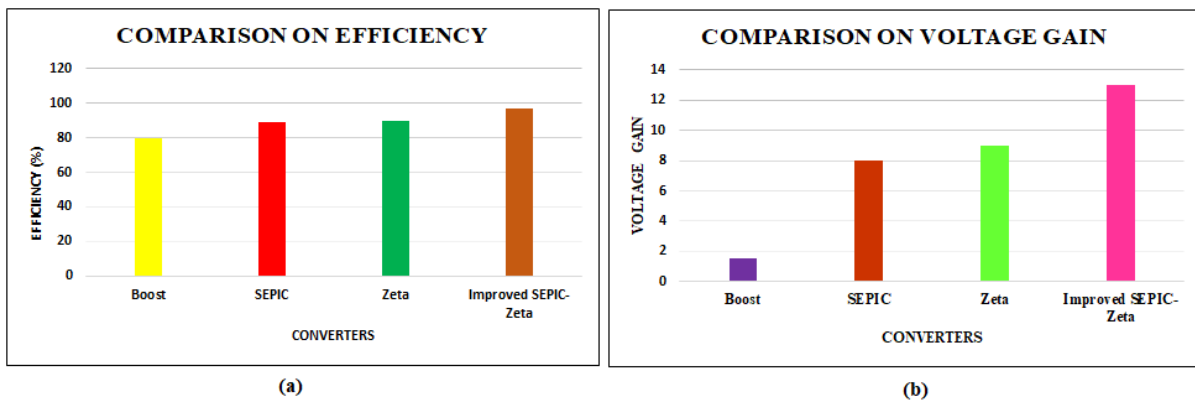


Figure 15: Comparison analysis (a) Efficiency (b) Voltage Gain

Figure 16 illustrates comparison for THD for different existing converters with proposed improved SEPIC-Zeta converter. THD has an effect on the power system because it results from any deviation in the sinusoidal waveform that PWM creates. When compared to alternatives, this converter exhibits reduced distortion in harmonics. It is possible to further reduce THD by applying a filter across the load.

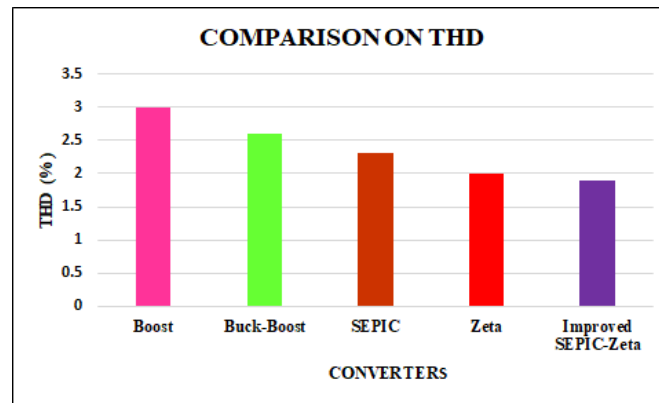


Figure 16: Comparison for THD values

V. CONCLUSION

The adoption of EVs has recently increased quickly due to their decreased greenhouse gas emissions, improved air quality, and less impact on urban climate conditions. Additionally, they use electricity instead of fossil fuels like diesel and gasoline. Hence, EV battery monitoring is crucial for the better usage of battery charged vehicles whenever required. In this work, IoT platform is utilized for monitoring the voltage and current obtained from PV system and battery SOC. Improved SEPIC-Zeta converter is employed for enhancing the power received from PV cells and Modified LOA is utilized to obtain optimized power output which is further supplied to grid. Overall system is executed in MATLAB Simulink and proposed converter is compared with existing approaches. From the comparison, it is observed that the efficiency and voltage gain obtained are 97% and 1:13 respectively. The distortion attained in the waveforms is minimized with range of 1.89% that is lower than other converter approaches.

REFERENCES

1. M. H. Mobarak, R. N. Kleiman, and J. Bauman, "Solar-charged electric vehicles: A comprehensive analysis of grid, driver, and environmental benefits," *IEEE Trans. Transport. Electrific.* vol. 7, no. 2, pp. 579–603, Jun. 2021.
2. K. S. Kavın & P. Subha Karuvelam (2021): PV-based Grid Interactive PMBLDC Electric Vehicle with High Gain Interleaved DC-DC SEPIC Converter, *IETE Journal of Research*, Sept. 2018.
3. Liu, K., Hu, X., Wei, Z., Li, Y., Jiang, Y. Modified gaussian process regression models for cyclic capacity prediction of lithium-ion batteries. *IEEE Transactions on Transportation Electrification* 2019; 5 (4):1225–1236.
4. Hu, X., Liu, W., Lin, X., Xie, Y. A comparative study of control oriented thermal models for cylindrical li-ion batteries. *IEEE Transactions on Transportation Electrification* 2019; 5 (4):1237– 1253.
5. Hejazi, H., Taylor, Z., Mohsenian-Rad, H. Optimal cell removal to enhance operation of aged grid-tied battery storage systems. *IEEE Transactions on Sustainable Energy* 2020; 12 (1):1–1.
6. M. A. Devlin and B. P. Hayes, "Non-intrusive load monitoring and classification of activities of daily living using residential smart meter data," *IEEE Trans. Consum. Electron.* vol. 65, no. 3, pp. 339–348, Aug. 2019.
7. M. Veerachary and P. Kumar, "Analysis and Design of Quasi-Z-Source Equivalent DC–DC Boost Converters," in *IEEE Transactions on Industry Applications*, vol. 56, no. 6, pp. 6642-6656, Nov.-Dec. 2020.
8. S. Hasanpour, A. Baghrmian and H. Mojallali, "Analysis and Modeling of a New Coupled-Inductor Buck–Boost DC–DC Converter for Renewable Energy Applications," in *IEEE Transactions on Power Electronics*, vol. 35, no. 8, pp. 8088-8101, Aug. 2020.
9. S. Miao and J. Gao, "A Family of Inverting Buck-Boost Converters With Extended Conversion Ratios," in *IEEE Access*, vol. 7, pp. 130197-130205, 2019.

10. A. Anand and B. Singh, "Modified Dual Output Cuk Converter-Fed Switched Reluctance Motor Drive With Power Factor Correction," in *IEEE Transactions on Power Electronics*, vol. 34, no. 1, pp. 624-635, Jan. 2019.
11. R. Kushwaha and B. Singh, "A Power Quality Improved EV Charger With Bridgeless Cuk Converter," in *IEEE Transactions on Industry Applications*, vol. 55, no. 5, pp. 5190-5203, Sept.-Oct. 2019.
12. B. Zhu, G. Liu, Y. Zhang, Y. Huang and S. Hu, "Single-Switch High Step-Up Zeta Converter Based on Coat Circuit," in *IEEE Access*, vol. 9, pp. 5166-5176, 2021.
13. Y. P. Siwakoti et al., "High-Voltage Gain Quasi-SEPIC DC–DC Converter," in *IEEE Journal of Emerging and Selected Topics in Power Electronics*, vol. 7, no. 2, pp. 1243-1257, June 2019.
14. H. Zhao *et al.*, "Shielding Optimization of IPT System Based on Genetic Algorithm for Efficiency Promotion in EV Wireless Charging Applications," in *IEEE Transactions on Industry Applications*, vol. 58, no. 1, pp. 1190-1200, Jan.-Feb. 2022.
15. C. Zhang *et al.*, "Dedicated Adaptive Particle Swarm Optimization Algorithm for Digital Twin Based Control Optimization of the Plug-In Hybrid Vehicle," in *IEEE Transactions on Transportation Electrification*, vol. 9, no. 2, pp. 3137-3148, June 2023.
16. T. Khurshaid, A. Wadood, S. Gholami Farkoush, J. Yu, C. -H. Kim and S. -B. Rhee, "An Improved Optimal Solution for the Directional Overcurrent Relays Coordination Using Hybridized Whale Optimization Algorithm in Complex Power Systems," in *IEEE Access*, vol. 7, pp. 90418-90435, 2019.
17. X. Liang and C. Andalib -Bin- Karim, "Harmonics and Mitigation Techniques Through Advanced Control in Grid-Connected Renewable Energy Sources: A Review," in *IEEE Transactions on Industry Applications*, vol. 54, no. 4, pp. 3100-3111, July-Aug. 2018.
18. H. Du, Q. Yang, X. Dai, X. Liao and A. Zhang, "A Parameter Extraction Method for LC Circuit of DB-BPF Based on Fully Connected Network," in *IEEE Transactions on Computer-Aided Design of Integrated Circuits and Systems*, vol. 41, no. 10, pp. 3558-3562, Oct. 2022.
19. Nejabatkhah, Farzam, Saeed Danyali, Seyed Hossein Hosseini, Mehran Sabahi, and Seyedabdolkhalegh Mozaffari Niapour, "Modeling and control of a new three-input DC–DC boost converter for hybrid PV/FC/battery power system," *IEEE Transactions on power electronics*, vol. 27, no. 5, pp. 2309-2324, 2011.
20. Javeed, Patan, Lochan Krishna Yadav, P. Venkatesh Kumar, Ranjit Kumar, and Shakti Swaroop, "SEPIC Converter for Low Power LED Applications," In *Journal of Physics: Conference Series*, vol. 1818, no. 1, p. 012220. IOP Publishing, 2021.
21. Saravanan, S., P. Usha Rani, and Mohan P. Thakre. "Evaluation and Improvement of a Transformerless High-Efficiency DC–DC Converter for Renewable Energy Applications Employing a Fuzzy Logic Controller." *MAPAN* (2022): 1-20.